UNIVERSITÉ DU QUÉBEC

MÉMOIRE PRÉSENTÉ À
L'UNIVERSITÉ DU QUÉBEC À TROIS-RIVIÈRES

COMME EXIGENCE PARTIELLE DE LA MAÎTRISE
EN SCIENCES DE L'ÉNERGIE ET DES MATÉRIAUX
OFFERT EN EXTENSION
PAR L'INSTITUT NATIONAL DE LA RECHERCHE SCIENTIFIQUE

PAR
AMALA MARY JOSE

ALKALINE AQUEOUS REFORMING OF CELLULOSE TO PRODUCE HIGH PURITY HYDROGEN WITHOUT CO_x

DÉCEMBRE 2013

Résumé

Notre objectif est de développer un dispositif expérimental pour produire de l'hydrogène à partir de biomasse cellulosique sans aucune émission de CO_2 par une technologie de reformage en milieu alcalin aqueux. Le principe du procédé est essentiellement de recombiner la teneur en carbone de la biomasse via une réaction chimique pour former des carbonates et donc de libérer l'hydrogène dans a forme pure. L'hydrogène produit est pur à ≥95 % et peut être utilisé directement dans certaines applications. La teneur en humidité de la biomasse ne modifie pas le procédé puisque de l'eau est nécessaire pendant le processus de conversion, évitant ainsi le besoin de sécher la biomasse. La réaction chimique décrivant ce procédé est :

$$(C_6H_{10}O_5)_n + 12n\ NaOH + n\ H_2O \xrightarrow{Ni/Al\text{-}Si} 6n\ Na_2CO_3 + 12n\ H_2O \qquad (1)$$

Cette réaction est optimum à des températures entre 300 et 350 °C. Le processus a été réalisé en présence de Ni pure (~ 0,3 micron, 99%) et supporté (Ni/Al-Si) comme catalyseur avec différentes concentrations alcalines afin de comparer la production d'hydrogène dans sous différentes conditions. Une étude du bilan de masse est également menée et le nombre de moles d'hydrogène produit est calculé en utilisant l'équation des gaz parfaits. Les sous-produits obtenus après la gazéification ont été analysés quantitativement et qualitativement par diffraction des rayons X (XRD), spectroscopie Raman et par titrage à double indicateur du sel. Afin de minimiser le coût des catalyseurs et apporter une valeur ajoutée aux produits dérivés, le catalyseur doit être récupéré et activé pour des réactions consécutives. L'étude de la récupération du catalyseur (Ni) a été effectuée et nous concluons que la sédimentation et la séparation magnétique se sont avérées des méthodes efficaces pour la séparation du Ni supporté et pur. Notre solution à base de 10 % de NaOH et de 90 % de Na_2CO_3 nous apporte un rendement de catalyse de 95 % à partir d'une solution à base de 10 % de NaOH et de 90 % de Na_2CO_3 à l'aide de méthodes de séparation du Ni.

L'ensemble de notre étude expérimentale est classé en trois phases, car nous avons dû utiliser trois réacteurs différents. Les deux premiers ont développé des fissures en raison

de problèmes occasionnés par la fragilisation caustique et le « stress corrosion cracking » causé par l'hydrogène. Nous avons choisi l'INCONEL®600 (nickel-chrome-fer) comme matériau de fabrication pour le troisième réacteur. Ce matériel résiste à la corrosion avec des solutions caustiques à haute température et au phénomène de « stress corrosion cracking » causé par l'hydrogène.

Une production de gaz correspondant à une élévation de la pression finale de 10 psig, qui constitue 95% d'hydrogène, est obtenue à partir de 1 g de biomasse cellulosique et l'efficacité du système est estimée à 52,30 %. L'analyse quantitative par l'utilisation de titrage à double indicateur montre une présence de 2,67 g de carbonate de sodium et 0,62 g de soude dans la solution sous-produit, et donc le rendement de conversion de l'hydroxyde de sodium en carbonate de sodium est de 68,10%. La solution de sel est qualitativement analysée par diffraction des rayons X et spectroscopie Raman et identifie la présence de carbonates. Le sous-produit de la gazéification, la soude, est largement utilisé dans les industries du verre, dans la fabrication de produits chimiques tels que le bicarbonate de soude et d'autres composés contenant du sodium, la désulfuration de gaz et en blanchiment des pâtes dans l'industrie du papier.

Abstract

Hydrogen is produced from cellulosic biomass without any CO_x emissions using a novel aqueous alkaline reforming (AAR) technology. The principal advantage of this process is that theoretically, all the carbon in the biomass is converted into sodium carbonate (Na_2CO_3), a product of commercial value. The moisture content in the biomass feedstock does not affect the process, as water is needed during the conversion process, thus avoiding the need to dry the biomass. The runs were conducted with different concentrations of sodium hydroxide and both supported (Ni/Al-Si) and pure Ni (~ 3 micron, 99.7%) catalysts were used to compare the H_2 production under different conditions. The gas produced was analyzed using a gas chromatography and the number of moles of hydrogen produced was calculated using the real gas equation. Our experimental results showed that hydrogen with a purity of $\geq$ 95 % was produced with no traces of either CO or CO_2, at temperatures as low as 300 – 350 °C, with 2 M NaOH, in presence of supported Ni catalyst. Mass balance study was conducted by qualitative and quantitative analyses of the by-products using XRD, Raman spectroscopy and double indicator titration. The catalyst used for the gasification reaction could be recuperated and sedimentation and magnetic separation were proven to be effective methods for recuperation of supported Ni (Ni/Al-Si) and pure Ni catalysts respectively.

Acknowledgement

I would like to thank Lord Almighty for showering his blessings upon me to fulfill my studies and would gladly surrender my work under his majesty. Without his grace and guidance I would not have attained it.

I would like to thank my parents who provided me a great support and encouragement in my academic as well as in my day to day life.

I am so grateful to my thesis director, Professor Jean Hamelin, for providing me such a wonderful opportunity to work under him which gave me an immense opportunity to learn different aspects and a great academic exposure. It was a great experience for me to work under his enthusiastic supervision and motivation.

I would express my sincere gratitude to Sadesh Kumar Natarajan who supported me during my project. I thank him for providing me a good environment and facilities to complete the project.

I would like to thank Robert Drolet and Daniel Cossement for their kind helping hand.

My sincere gratitude to Renju Zacharia for his technical guidance and wise suggestions.

I express my sincere thanks to my colleague Paul-André for his wonderful co-operation in the project.

I extend my thanks to my colleague Siyad Ubaid and Francis Lafontaine for the encouragement and support.

Last but not the least let me thank the funding agency, H2CAN for providing a great financial support throughout the project, which made it possible.

I also place on record, my sense of gratitude to one and all, who directly or indirectly, have lent their helping hand in this venture.

Table of Content

List of Figures

List of Tables

1. Introduction

Global warming is rising at an alarming rate and the earth's temperature is projected to rise another 2 to 11 °F over the next hundred years [1]. Human activities such as fossil fuel utilization, deforestation and industrial processes contribute significantly to the release of greenhouse gases. Greenhouse gases act like a blanket that traps the infrared radiation in the atmosphere and hence causing it to warm thus increasing the global temperature. There is a huge demand for clean energy to protect the environment from the deleterious effects of global warming and hydrogen energy offers significant potential in this scenario as it is a clean and efficient energy. Hydrogen is considered as the fuel of the future mainly due to its high conversion efficiency, recyclability and non-polluting nature [2] as hydrogen combustion produces water. It has the advantage of highest energy density and safety which can supply tremendous power for stationary as well as transportation markets.

A key point related to hydrogen for energy production is that it is a substance that is not "found" like cru de oil or natural gas, but rather "made" like electricity from one of many different means. Hence it is considered as an energy carrier rather than an energy source [3]. Hydrogen usage is highly demanded in applications based on fuel cell technology along with other ways to use hydrogen for electricity production or energy storage. More than 50 types and sizes of commercial fuel cells are being sold, and the value of fuel cell shipments reached 498 million dollars in 2009 [3]. However, for fuel cell applications a high level of hydrogen purity is typically more important than for many industrial applications and thus can often entail higher costs of delivery. Vehicles can be powered with hydrogen fuel cells, which are three times more efficient than a gasoline-powered engine [4]. Globally, the hydrogen production figure is 50 M tonnes/year [5] and the major current uses of the commercially produced hydrogen are ammonia synthesis, oil refining [6], where hydrogen is used for hydro-treating of crude oil as part of the refining process to improve the hydrogen to carbon ratio of the fuel, food production (e.g., hydrogenation), treating metals, and producing ammonia for fertilizer and other industrial uses.

Global hydrogen production technologies can be widely divided into 3 groups, (1) thermal, (2) electrolytic, and (3) fermentation and photolytic processes [7]:

(1) Thermal processes include reforming of natural gas (steam methane reforming, partial oxidation), gasification of coal, gasification of biomass, reforming of renewable liquid fuels, and high temperature water splitting;
(2) Electrolytic processes include PEM electrolyzers, alkaline electrolyzers, and solid oxide electrolyzers;
(3) Fermentation comprises dark and photo fermentation in which hydrogen is produced from organic compounds by bacterial action. Photolytic processes include photo-biological water splitting and photo-electrochemical water splitting.

The production of hydrogen from fossil fuels causes the co-production of carbon dioxide (CO_2), which is assumed to be the main responsible for the so-called 'greenhouse effect' [8].

The capture of CO_2 for storage purposes is not yet technically and commercially proven and requires further R&D on absorption or separation processes and process line-up. A high-temperature electrolysis process is feasible only when high temperature heat is available as waste heat from other processes and also it requires R&D in materials development for solid-oxide fuel cell (SOFC) [9].Even though water electrolysis is a proven technology for hydrogen production, it is not quite cost competitive. The other processes for hydrogen production such as photo-electrolysis and photo-biological processes are further away from commercialization and need additional R&D [9].

The United States Department of Energy (DEO) has set certain clean energy goals for the upcoming years such as reduction of greenhouse gas (GHG) emissions and petroleum use 50% by 2030, reduce GHG emissions 83% by 2050, invest 150 billion dollars over 10 years in energy R&D to transition to a clean energy economy [10]. Hence there is a great emphasize to shift the hydrogen production pathways towards renewable sources of energy to reduce the environmental impact and thus to pave way towards a clean energy. Hydrogen produced through a range of renewable primary energy sources such as wind, biomass, and solar energy is ideal for gradually replacing fossil fuels [11]. Biomass was the major source of energy during the 19^{th} century, which has been taken over by fossil fuel based economy in the later stages due to low biomass to energy conversion efficiency.

But with increasing industrialization the energy demands are so high that it requires a shift back towards biomass based economy due to two major reasons; first, it is a sustainable source of renewable energy, eco-friendly with very less CO_2 emission and second, the high rate of depletion of fossil fuels. Biomass energy potential is addressed to be the most promising among the renewable energy sources, due to its spread and availability worldwide [12]. The benefits of a true hydrogen economy can only be achieved if the hydrogen is derived from renewable and carbon neutral resources like biomass. Biomass, especially organic waste, offers an economic, environmental friendly way for renewable hydrogen production [13].

Canada has a great potential of forestry and agricultural resources to provide a renewable and sustainable supply of bio-based energy. Canada generates approximately 1.45×10^{8} t of residual biomass per year, containing an estimated energy value of 2.28×10^{9} GJ, which is equivalent to about 22% of Canada's current annual energy use. Conversion of these residues using emerging technologies that favor the synthesis of H_2 and represses the synthesis of CH_4 could generate 1.47×10^{10} m^3/year of renewable H_2, with a heating value of 1.89×10^{8} GJ [14].Thus hydrogen production from biomass has a significant role in building up a clean energy economy for a biomass rich developed country.

The objective of the project was to develop an experimental set-up to produce hydrogen from cellulose biomass without any CO_2 emission by an aqueous alkaline reforming technology. The principle behind the process is basically that the carbon content from the biomass combines with aqueous alkali to form carbonates and hence releases hydrogen in its pure form. The produced hydrogen is $\geq$ 95% pure and does not require much purification to be used in other applications. The moisture content of the biomass does not affect the process as water is needed during the conversion process, thus avoiding the need to dry the biomass. The process has been carried out in presence of pure (0.3 micron, 99%) and supported Ni (Ni/Al-Si) and under different alkaline concentrations to compare the hydrogen production under different conditions. A mass balance study was also conducted and the number of moles of hydrogen produced was calculated using the real gas equation. The by-products obtained after the gasification were analyzed both qualitatively and quantitatively by XRD, Raman spectroscopy and double indicator salt titration.

The recuperation study for the Ni catalysts was also carried out and it was found that sedimentation and magnetic separation proved to be the effective methods for the separation of supported and pure Ni respectively from the gasified sample.

The entire experimental study was classified into three phases as the work was performed in three different batch reactors due to issues such as caustic and hydrogen embrittlement and stress-corrosion cracking. The third phase of batch reactor constructed with a suitable material was found successful for the aqueous alkaline reforming of biomass for hydrogen production.

2. Reaction Stoichiometry & Role of reactants

Stoichiometry

In the following chemical reaction [15]:

$$(C_6H_{10}O_5)_n + 12n\ NaOH + n\ H_2O \text{ -----> } 6n\ Na_2CO_3 + 12n\ H_2O \quad (1)$$

as per the stoichiometry 1 mol of cellulose (162 g) reacts with 12 mols of NaOH (480 g) and 1 mol of H_2O (18 g) in presence of Ni catalyst to produce 6 mols of Na_2CO_3 (636 g) and 12 mols of H_2 (12×2.016 g). The mole ratio of carbon in biomass to alkali metal hydroxide is 1:2. Hence based on the carbon content in different types of cellulose, required quantity of alkali metal hydroxides is added. The ratio of biomass wt. to catalyst wt. is 2.5:1.The runs were conducted with Ni supported on Al-Si (65 wt.%) as well as with pure Ni catalyst (99.7%).

Role of reactants

NaOH: - There is a competition between the dehydration pathway and the gasification pathway for the biomass hydrolysis products. The end product of dehydration route is char, tar, hydrocarbon gases, while the end product of gasification route is mainly hydrogen [16]. In the absence of alkali, dehydration and decarboxylation is favored and biomass hydrolysis products conversion to tars and chars occurs with CO_2 production. Tar and char formations involve the formation of furfural and 5-hydroxymethylfurfural (5HMF) from biomass compounds which are formed during the early dehydration of biomass molecules. In the presence of alkali, the dehydration pathway is suppressed as the water-soluble compounds are sustained in solution which favors the gasification route owing to the conversion of biomass to simple carbonyl compounds which further promotes hydrogen production. Alkali promotes hydrogen production by capturing the CO_2 produced and accelerating water-gas shift reaction. It is an effective method in breaking the ester bonds between lignin, cellulose and hemicellulose and avoids fragmentation of hemicellulose polymers. Addition of NaOH also causes lowering of operating temperature and hence reduces consumption of heat [17].

The hydrogen gas yield in relation to the alkali catalyst follows the order [18]:

$$NaOH>KOH> Ca(OH)_2 >K_2CO_3 >Na_2CO_3 >NaHCO_3.$$

Ni - The addition of Rh, Ni, Ru, or Co catalysts decreased the formation of methane and increased the formation of hydrogen. The total yields of hydrogen were higher in the order of Rh/Al_2O_3, Ni/Al_2O_3, Ru/Al_2O_3, Co/ Al_2O_3 > Pd/ Al_2O_3 > Pt/ Al_2O_3 > Cu/ Al_2O_3 > Fe/Al_2O_3. Ni, Co, Rh, and Ru catalysts promote cleavage of C-H bonds of cellulose derivatives, reaction intermediates, and desorption of H species as H_2 to the gas phase. Therefore, the methane formation was significantly suppressed and the hydrogen formation was accelerated at low temperatures [19].

H_2O - Water added in excess serves as a medium for the chemical reaction to occur as well as to reduce the charring process. It suppresses the dehydration pathway and promotes the gasification pathway for hydrogen production. The use of steam, instead of air or CO_2, leads to higher H_2 yields due to the additional H_2 produced from the decomposition of H_2O. Water has a catalytic role in various acid/base catalyzed processes due to its higher degree of ionization at the increased temperature. According to the transition state theory, the presence of water in some organic reactions (also some hydrolysis and decarboxylation reactions) can cause a decrease of the activation energy, thus affecting the kinetic of the reaction [20].

3. Experimental Procedure

The thermochemical gasification of biomass was conducted in three phases of study. In the first two phases, the gasification was carried out in a stainless steel reactor with different heating modes and in the third phase the gasification was performed in a reactor made of Inconel® Alloy-600, a Ni-based carbon free alloy. This Ni-based alloy offers high resistance to caustic stress corrosion cracking and hydrogen embrittlement compared to stainless steel.

Phase 1

In this phase, a stainless steel (SS) reactor was built from a SS-316 hollow bar based on the flange model. A batch reactor of 442 mL was built from a hollow bar of SS-316 with the dimensions 5.5" (13.97 cm) height , 4" (10.16 cm) outer diameter and 2.5" (6.35 cm) inner diameter. Bottom flange was welded on to the reactor mouth and top flange was bolted using 16 nuts. The top flange of the reactor consisted of feeding tube, gas inlet tube and gas outlet tube. The bottom of the cylinder was closed by a thick plug welded to a thickness of about 0.635 cm (0.25"). The feed from the feed hopper was introduced into the reactor using a steam service ball valve model SS-S65PS16 from Swagelok. Figure 1 shows different parts of the reactor under construction.

Figure 1: SS-316 reactor under construction.

The reactor was heated using three high density cartridge heaters (400 W, 120 V) connected in parallel. The wiring schematic is given in Appendix B. It was inserted into

the reactor wall by making three holes of appropriate diameter on the reactor wall. The reactor was provided with K-type thermocouples (1/8" SS tube well) and a high temperature pressure transducer for acquiring temperatures and pressures. Temperature of the reactants and the produced gas were acquired using bore through compression fittings which were inserted inside the reactor through the reactor surface. Temperature of the reactor was monitored real time at various points such as at the feed inlet, at the level of the produced gas, and at the reactor wall. The batch reactor and its different parts are shown in Figure 2 and the complete set-up can be seen in Figure 3.

Experimental runs were performed in 2 different ways. Initially the reactants were filled inside the feed hopper, sparged with Ar and held by the closure of a ball valve. The reactor alone was heated from room temperature to 300 °C and once it reached the desired temperature the ball valve was opened and the reactants were pushed into the reactor. But since the reactants were in the form of slurry a good portion of it got stuck inside the ball valve and hence the reaction was not complete. For the second run, the reactants were introduced inside the reactor, the reactor was closed air tight, purged with Ar to make the reactor O_2-free and then heated the reactor to 300 °C. The initial pressure was 20 psig of Ar and the runs were performed with 5 g of cellulose biomass as the feed stock. As per the stoichiometry 5 g of cellulose reacts with 14.8 g of NaOH and excess H_2O (50 mL) in presence of Ni/Al-Si (2 g) catalyst. The 14.8 g of NaOH in 50 mL H_2O constitutes a 7.4M solution. Before the experimental runs, blank runs of pure H_2 and Ar gases were performed to understand the thermal expansion and behaviour of H_2 and Ar at high temperatures. The reactor was insulated with Al foil backed ceramic insulation fiber to minimize the heat transfer to surroundings by convection. The reactor was heated to 300 °C and held for a retention time (RT) of 30 min. After the retention time the power was switched off and the system was allowed to cool down to room temperature. The reactor was cooled to condense the water vapour formed and hence to exclude the pressure produced from water vapour formation and it also allows the thermally expanded Ar to revert to its initial pressure.

Overtime a leak was developed on the reactor wall where the bore through thermocouples were inserted due to high pressure formation inside the reactor as a result of gasification experiment. High temperature silica containing sealant paste (Deacon 770P) was used to seal the leak between the reactor wall and the thermocouple but the paste proved inadequate due to the presence of silica in the paste which is not advisable to use with strong acids and alkalis. In the later stages a crack was observed on the reactor wall near the thermocouple welded area and it has been concluded that welding of the thermocouples should be avoided on curved surface under extreme conditions and harsh chemical environment. Welding is preferred on the flat surfaces like top or bottom for a high pressure reactor. Figure 4 shows the leak from the bore through thermocouple fitting and Figure 5 shows the crack formation on reactor wall.

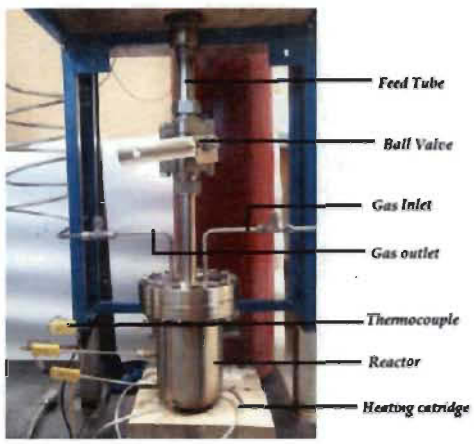

Figure 2: Batch reactor (SS-316)

Figure 3: The reactor set-up for thermochemical gasification of cellulose.

Figure 4: Leak from bore through thermocouple welding.

Figure 5: Crack formation on the reactor wall.

Phase 2

The second phase of the experiment was performed using SS-316 high pressure reactor of 1337 mL volume from Parr Instruments. For the second setup, the same reactants were used as in Phase 1 (5 g cellulose and 7.4M NaOH) but with different heating modes for the reactor. The experimental runs were performed under the same conditions of temperature and initial pressure as in Phase 1; 300 °C and 20 psig Ar. The reactor is shown in Figure 6.

The reactor was heated using an ultra-high temperature tape heater with 1400 W capacity. The reactor was insulated with Al foil backed ceramic insulation fiber to minimize the heat transfer to surroundings by convection. The reactor was then allowed to cool down to room temperature. A leak was observed during the cooling process due to melting of the gasket. The gasket used was high temperature PTFE (poly tetra fluroethylene polymer) which could withstand temperatures up to 350 °C. But with long retention times, melting of the gasket occurred and hence the reactor had to be modified to use a metal (Cu) gasket. The leak issue was fixed with modification and the heating mode was improved by replacing tape heater with the mica insulated band heater (1200 W). The temperature of the reactor was monitored at the reactor wall and at the heating element. After few runs a crack developed at the bottom of the reactor which resulted in the gas leak and these shows that if steel is exposed to hydrogen at high temperatures, hydrogen will diffuse into the alloy and combine with carbon to form tiny pockets of methane at internal surfaces like grain boundaries and voids. This methane does not diffuse out of the metal, and collects in the voids at high pressure and initiates cracks in the steel. This selective leaching process is known as high temperature hydrogen attack and leads to decarburization of the steel and loss of strength and ductility [21].Thus stainless steel reactors are highly prone to caustic and hydrogen embrittlement and stress-corrosion cracking in presence of strong alkalis.

Figure 6: SS-316 Parr Instruments reactor

Phase 3

Selection of material

As cracks developed in both of the stainless steel reactors during the thermochemical gasification process, literatures [22-25] were reviewed to find a suitable material for reactor construction. It was found that resistance to stress corrosion cracking (SCC) and general corrosion in NaOH solutions and molten NaOH improves as nickel content increases in Fe-Ni-Cr, Ni-Cr-Fe and Ni-Cr-Mo alloys. This is due to the ability of nickel to form protective oxides in high pH environments. Nickel and Nickel alloys form several stable oxides or hydroxides at basic pH levels. The stable oxides and hydroxides formed by nickel at high pH levels provides a very protective passive film. The advantage of the low carbon grade in nickel is resistance to graphitization at elevated temperatures above 600°F (316 °C). In general, resistance to general corrosion and stress corrosion cracking increases with nickel content. Nickel alloys 200, 600 and 400 are common materials for handling hot concentrated caustic materials. The study shows that these alloys continue to exhibit good corrosion resistance at all concentrations of caustic NaOH (10%, 50% and 70%).

For high temperatures involving all concentrations of sodium hydroxide, one can use either the commercial pure ASME Standard SB-162 Nickel 200 or Nickel 201, with low-carbon Nickel 201 being better above 315 °C. These are relatively low strength alloys, so the reactor will have to be designed to handle the high pressures (for example, extra heavy walls). Alternative choices are nickel-chromium alloys like Alloy 600 (N06600) and

Alloy 625 (N06625), with the lower molybdenum containing alloy 600 having slightly better alkaline resistance. Both the ASME Standard SB-168 Alloy 600 and the ASME SB-443 Alloy 625 have good high temperature strength. Of all the above, Alloy 600 was found to be the best choice [23, 24] and was chosen as the material of choice for the reactor construction due to its beneficial effects in handling high concentration caustic and hydrogen embrittlement

Reactor designing

A batch reactor of Alloy-600 was designed and built with appropriate thickness and height to diameter ratio from a solid bar of Inconel® Alloy-600.

The design equations used to calculate the wall thickness t were [26, 27]:

$$t = PR/(SE - 0.6P), \qquad (2)$$

where P is the design pressure or maximum allowable working pressure (15 MPa = 2175 psi), R is the inside radius in inches (2 inches = 50.8mm), S is the stress value of the material, psi (10.6ksi =10600psi) [23], and E is the joint efficiency (0.85) [23]. The wall thickness in inches computes to

$$t = 2175\ \text{psi} \times 5.08/(10600\ \text{psi} \times 0.85 - 0.6 \times 2175\ \text{psi}) = 1.43\ \text{cm}.$$

From the perspective of safety and probability of future modification, the reactor was provided with a wall thickness of 1" (2.54 cm) and a head to diameter ratio of 1.75. Even though torispherical head is found to be the optimum design to deal with high pressure [27], the reactor was designed with a flat head for ease of construction.

A batch reactor of volume 1440 mL was built from a solid bar of Inconel® Alloy-600 with the dimensions of 7" height, 6" outer diameter and 4" inner diameter. Sixteen holes were drilled on the top of the reactor and the reactor lid was screwed on to the reactor using 16 bolts. Each bolt was given a torque of 30 lb ft to make the reactor leak-free at high pressures. Copper gasket of thickness 2.08 mm was used between the lids. The reactor was annealed at higher temperatures to relieve the stress and to make it resistant to stress corrosion cracking. The Alloy 600 reactor after heat treatment is shown in Figure 7.

The top flange of the reactors was fitted with a gas inlet and gas outlet tube and the inlet tube was connected to an Argon cylinder which purged the reactor to make it O_2-free before the reforming. After purging, the reactor was filled with 20 psig Argon before the heating began. The runs were conducted with 1 g of cellulose, 2.96 g of NaOH and Ni catalyst with excess water. The mass of feed was reduced to 1 g to reduce the pressure formation. The volume of water and amount of NaOH was varied to make the aqueous solution of alkali metal hydroxide into different concentrations such as 2 M (37 mL) and 4 M (18.5 mL). Lower concentrations of alkali metal hydroxides were chosen to avoid the caustic embrittlement and the stress-corrosion cracking of the reactor. The gasification was carried out with both supported and pure Ni (~ 3 micron, 99.7%) to compare the hydrogen formation in both cases. Prior to the experiments, biomass was mixed uniformly with an aqueous solution of alkali metal hydroxide.

The Alloy-600 reactor was heated using a ceramic insulated band heater of 1300 W capacity (Tempco-BCH7895). The temperature of the reactor was monitored at the reactor wall and at the heating element. The temperature of the reactor was regulated by a PID based on the data acquired by thermocouple fitted on to the heating element. The wiring schematic of PID (Omega, CN7533) with the solid state relay is given in Appendix B (parallel connected heaters need to be replaced by a band heater). As the temperature rose, the pressure increased inside the reactor and reached a stable value during the retention time. The set temperature of the PID was 350 °C for most of the runs and 400 °C for few other runs as the temperature regulation initiated 50 °C before it reached the set value for the PID controller. It took almost 1 h for the reactor to reach 300 °C from room temperature.

The temperature of the set-up was auto-regulated at the set value and the retention time of the reactor varies from 30 min to 1 h. The heating was cut off after the retention time and the reactor was allowed to cool down to condense the water vapour formed and hence to eliminate the pressure contributions from the water vapour formation and Ar expansion. Once the reactor attained the room temperature the pressure difference is noted from the initial pressure of Ar and the gas produced was analyzed using a MicroGC gas chromatograph. The gas produced as a result of the thermochemical gasification, takes its

way through the outlet tube. The reactors were provided with thermocouples and high temperature pressure transducer to monitor the temperature and pressure readings.

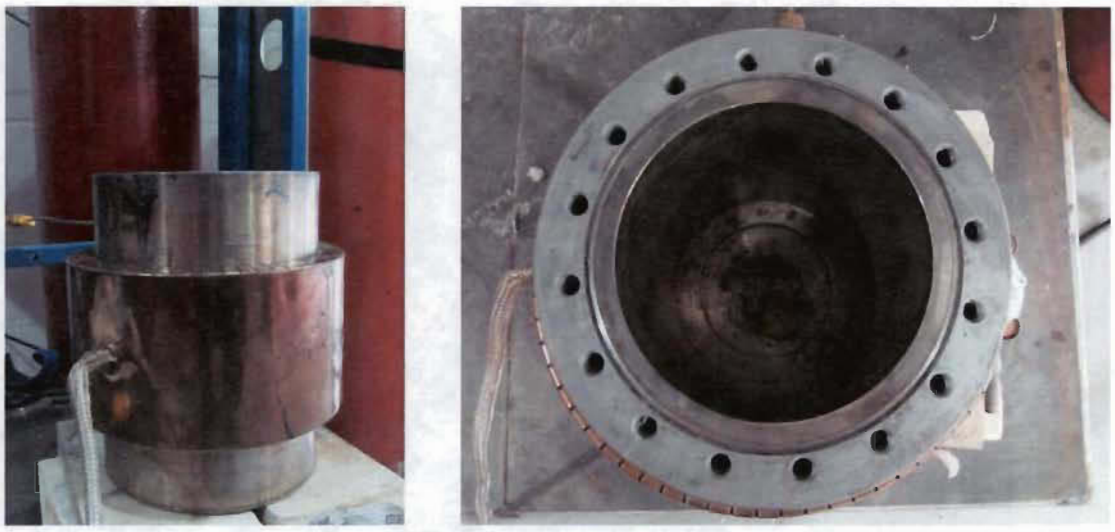

Figure 7: Alloy-600 reactor after heat treatment

4. Instrumental Set-up and Data Analysis

The data from the batch reactor system during the experimental run was acquired, monitored and real time graph plots were achieved using LabView version 9.0. Lab View served as the interface that allowed the measurement, test and control of the whole setup.

NI 9211(4 channel Thermocouple) and NI 9207(16 channel analog input) served as the input modules for the temperature and voltage-current (±10 V- ±21.5 mA) combination respectively. NI 9207 is powered externally by a 15 V power supply. It outputs the current in mA as per the pressure variation.

The MicroGC model 3000 from Agilent Technologies consists of a PLOT U column that detects carbon dioxide, ethylene, ethane, acetylene, and a MolSieve 5A column that detects neon, hydrogen, oxygen, nitrogen, methane and carbon monoxide. The MicroGC was calibrated for the detection of the above mentioned gases using Universal gas

calibration standard (Table 1) and Hydrogen-Carbon-dioxide-Carbon monoxide mixture from Praxair. Agilent Cerity software is used to control the MicroGC runs.

Table 1: Universal gas calibration standard

He	0.1000%
Ne	0.0496%
H_2	0.0988%
O_2	0.0500%
N_2	0.1000%
CH_4	Balance
Ethane	0.0497%
Ethylene	0.0497%
CO_2	0.0500%
CO	0.0995%
Acetylene	0.494%
Propane	0.0501%
Methyl Acetylene	0.0501%
n-Butane	0.0501%

The schematic of the entire set up is given in Figure 8 and the experimental set-up in Figure 9.

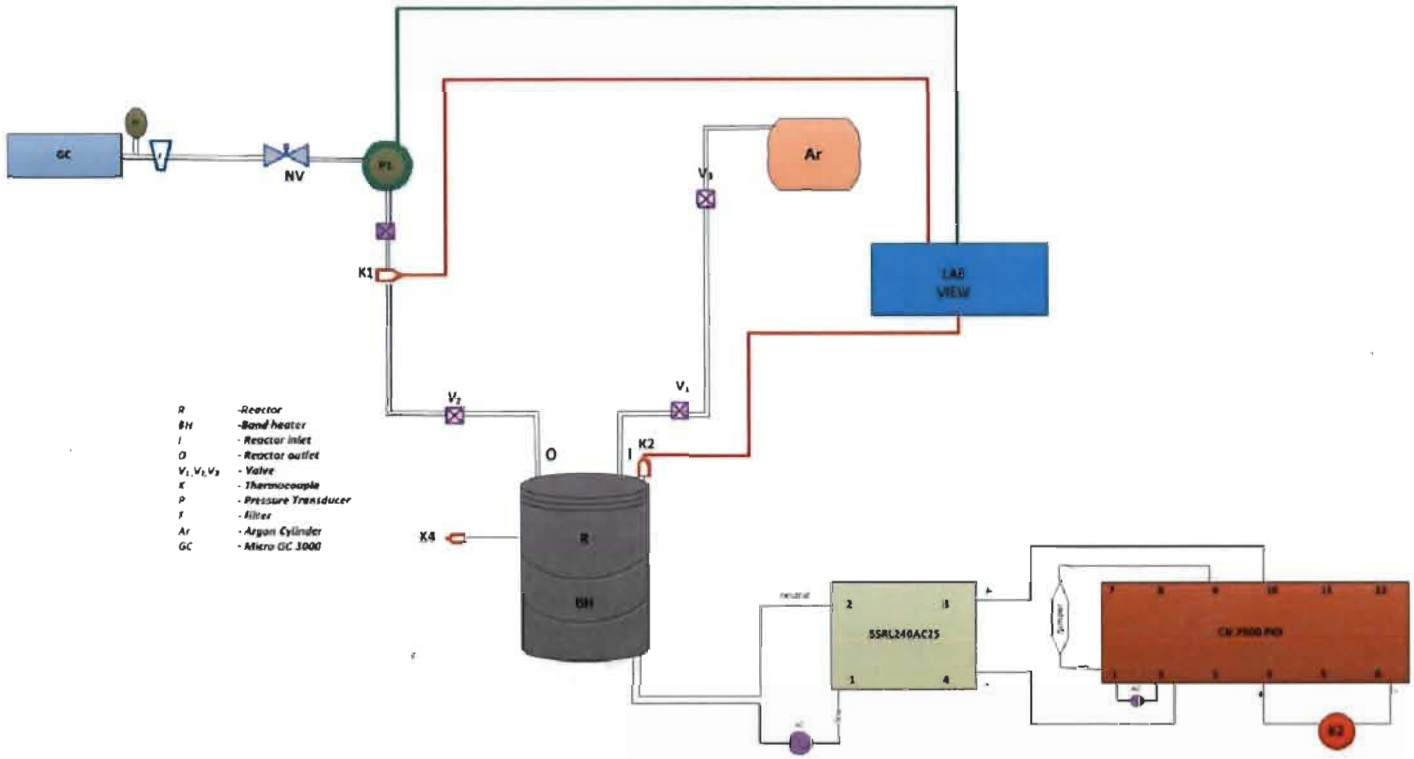

Figure 8: Schematic representation of the reactor setup

Figure 9: Experimental set-up of Alloy-600 reactor

5. Results & Discussions

Phase 1 (SS 316 - 442 mL)

Blank runs were performed in SS-316 reactor of 442 mL volume with pure H_2 and Ar samples before the experimental runs to study the thermal expansion and behaviour of gases at the temperature (300 °C) at which the thermochemical gasification occurs. The initial pressure of the Ar and H_2 were 50.57 psig and 50.89 psig respectively. It was found that pressure of both Ar and H_2 doubled at 300 °C. There was an increase from 50.57 psig to 102.21 psig for Ar and from 50.89 psig to 99.21 psig for H_2 as shown in Figure 10.a and Figure 10.b. This indicates that the pressure of the gas almost doubled on heating from room temperature to 300 °C.

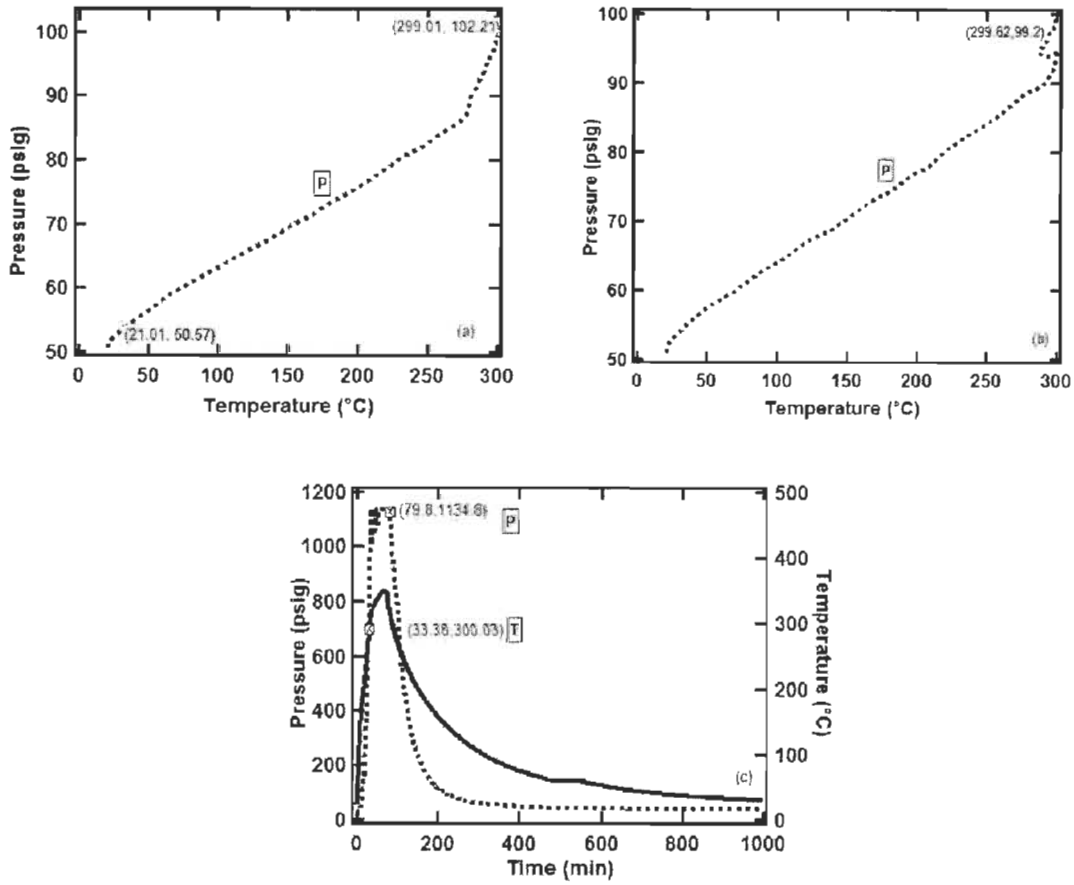

Figure 10: a) Pressure increase in blank run with Ar, b) Pressure increase in blank run with H_2, c) Pressure-Temperature profile of sample run

Experimental runs were performed with 5 g cellulose, 14.8 g of NaOH and excess H_2O (50 mL) in presence of Ni/Al-Si (2 g) catalyst with 20 psig Ar at the initial pressure. An exponential increase in pressure was observed with an increase in temperature and a graph of pressure and temperature vs. time is shown in Figure 10.c. The system attained 300 °C in 33 min and was held for a retention time (RT) of 30 min. The maximum pressure at the end of the retention time was 1134 psig. The cool down pressure went down to 36 psig as the reactor cooled, but a crack was observed on the reactor wall which leads to gas leak from the reactor.

Phase 2 (SS 316 - 1337 mL)

The SS-316 reactor from Parr Instruments was initially heated using a tape heater and later using a mica insulated heater. The reactants composition and initial pressure were same as in phase 1.

In run 1 which is showed in Figure 11.a, the reactor surface took only 5.47 min to reach 300 °C but the pressure inside the reactor after 5. 47 min reached only at 27.43 psig. Hence a longer retention time was provided for the conduction of heat from the heating element to inside the reactor and thus to improve the gasification rate and hence the pressure production. The maximum pressure developed inside the reactor was only 639.22 psig after providing a retention time of 2 h and 13 min.

In run 2 which is based on Figure 11.b, the reactor took 16.2 min to reach 300 °C but the pressure inside increased only up to 59.47 psig in 16 min. The maximum pressure developed inside the reactor after a retention time of 2 h and 49 min was only 599.81 psig.

The pressure production was less in either of the cases which indicates lower chemical reaction rate due to less efficient heating. During the heating process even though the surface of the reactor attained 300 °C rapidly the heat was not considerably transferred inside the reactor due to less heat of conduction from the heating element to the reactor surface. The conduction of heat was less due to the presence of air between the heating element and the reactor surface since the contact of heating element with the reactor surface was not air-tight. The trapped air in between had high insulation capacity which hindered the heat conduction to the reactor. Also the heat dissipation was found to be higher for tape heaters as the outer surface of tape heater is not provided with any further insulation unlike band heaters.

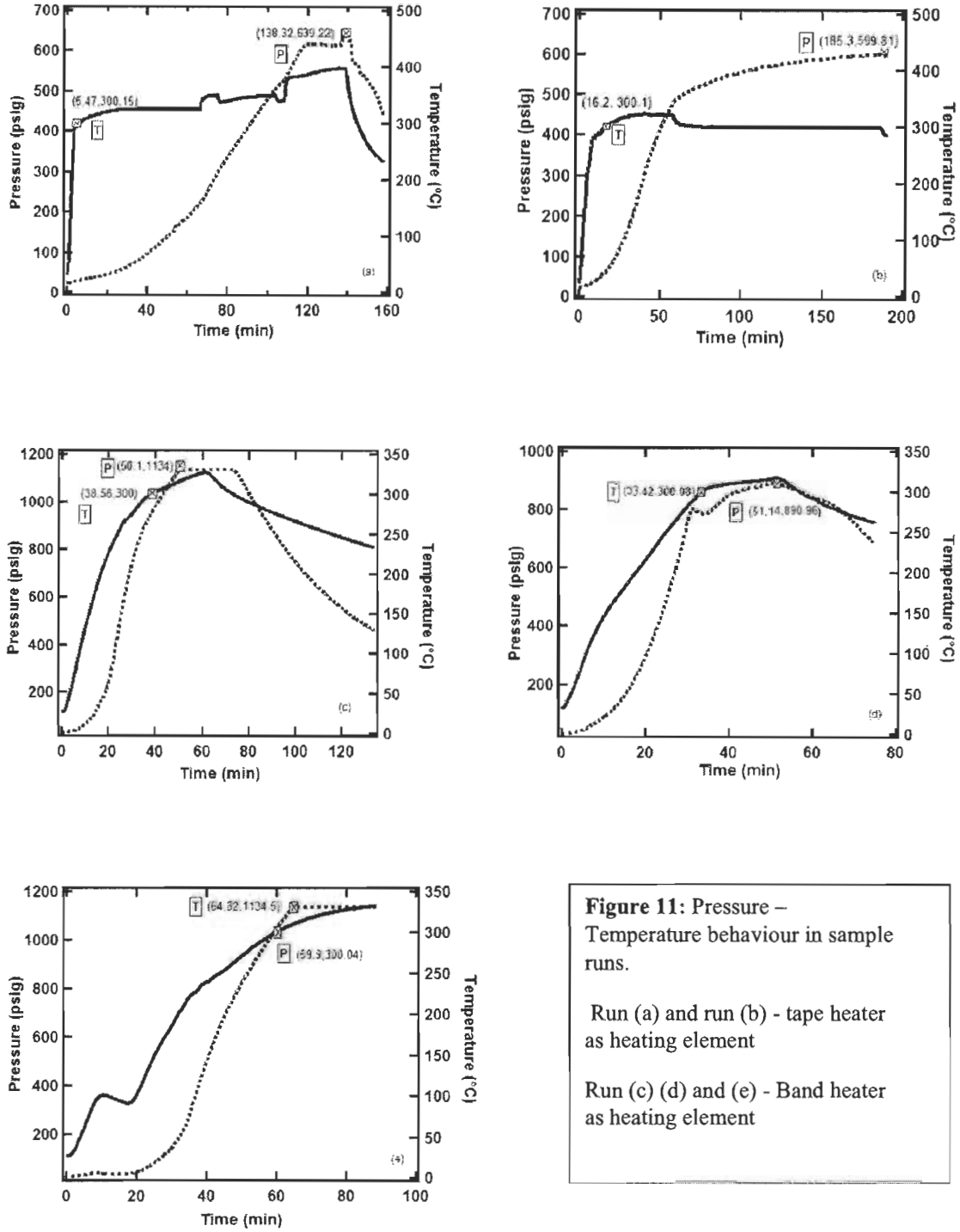

Figure 11: Pressure – Temperature behaviour in sample runs.

Run (a) and run (b) - tape heater as heating element

Run (c) (d) and (e) - Band heater as heating element

As the tape heater was found inefficient for heating the reactor to 300 °C, a band heater (1200 W) was chosen as the new heating element. The performance of the band heater is

quite better compared to the tape heater especially in the conduction of heat from the heating element to the reactor. As seen in Figure 11.c using band heater, the reactor reached 300 °C in 38 min and the maximum pressure the reactor reached was 1134 psig. The retention time of the reaction was 30 min.

In run d (Figure 11.d) the reactor reached 300 °C in 33 min and the maximum pressure the reactor reached was 890 psig. The retention time of the reaction was 30 min. Only 30 mL water was added in this run unlike others and hence final pressure produced was low compared to the previous run.

In the next run (Figure 11.e) the reactor reached 300 °C in 64 min and the maximum pressure the reactor reached was 1134 psig. The retention time of the reaction was 30 min. The difference in time consumption for the reactor to reach 300 °C may be due to poor insulation of the reactor in this case.

In all the above runs in phase 2 the final cool down pressure of the reactor was less than the initial pressure which indicates a leak was developed during the heating process and it was due to the inadequate reactor design to handle with high pressures. By the end of final run, a crack was also observed on the reactor bottom due to caustic embrittlement on stainless steel.

Phase 3 (Alloy 600 - 1440 mL)

The gasification was carried out in Alloy-600 reactor with 1g of cellulose, 2.96 g of NaOH in presence of supported and pure Ni catalysts. The initial pressure of Ar was kept at 20 psig. The volume of water used was 37 mL and 18.5 mL to constitute 2 M and 4 M NaOH respectively. The caustic concentration was kept low to protect the reactor from caustic embrittlement.

Figure 12 shows the temperature and pressure profile of the experimental runs, time taken for the reactor to attain 300 °C, the retention time and the maximum pressure developed inside the reactor at the end of retention time. The letter 'T' denotes the point at which the reactor attained 300 °C and 'P' is the point of max imum pressure production. It was observed reactor took an average time of 70 min to reach 300 °C and was given an

average retention time of 30-45 min after it reached the 300 °C, the desired temperature. The high pressure production was mainly contributed by the water vapor formation during the heating process and it varied between 800-1000 psig. The cool down pressures of the runs conducted with catalysts varied between 26-31 psig (Table 2).

Figure 12 (i-ii) are the runs performed using pure Ni catalysts whereas Figure 12(iii-vii) are the runs conducted with supported Ni catalysts. The pure Ni weighed 0.26 g which is equivalent to the weight percent of 0.4 g of supported Ni catalyst (65 wt.%). The reactor was given a retention time of 33 min in run (i) with 2 M NaOH and 48 min in run (ii) with 4 M NaOH after it attained 300 °C, the desired temperature. The maximum pressure produced in run (i) and (ii) were 862 psig and 524 psig respectively.

Figure 12 (iii, iv, v) are the runs conducted using supported Ni catalyst and 2 M NaOH which gave a maximum pressure production of 786 psig, 832 psig and 1005 psig respectively. Figure 12 (vi, vii) are the runs using supported Ni catalyst and 4 M NaOH and the maximum pressure produced were 828 psig and 536 psig respectively. The maximum pressure formation in run (ii) and run (vii) were less compared to other runs as they were performed with 18.5 ml of water unlike the other runs which were performed with 37 ml of water.

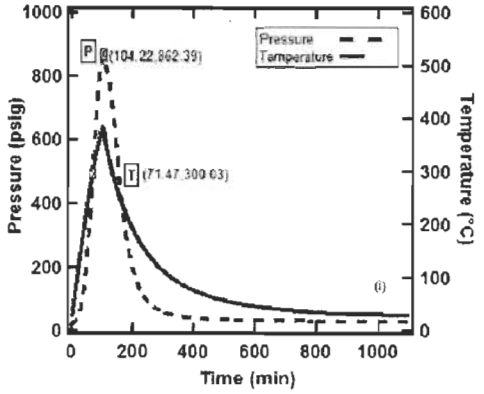
Pressure
Temperature
P (104.22,862.39)
T (71.47,300.03)
Pressure (psig)
Temperature (°C)
Time (min)
(i)

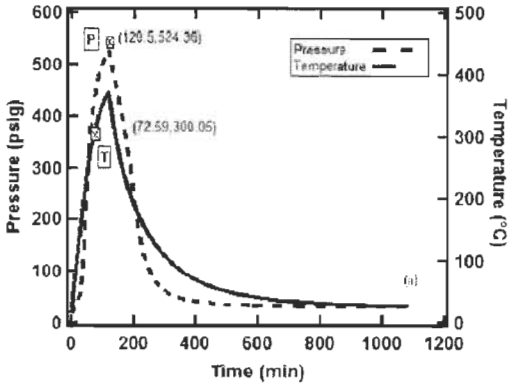
Pressure
Temperature
P (120.5,524.36)
(72.59,300.05)
T
Pressure (psig)
Temperature (°C)
Time (min)

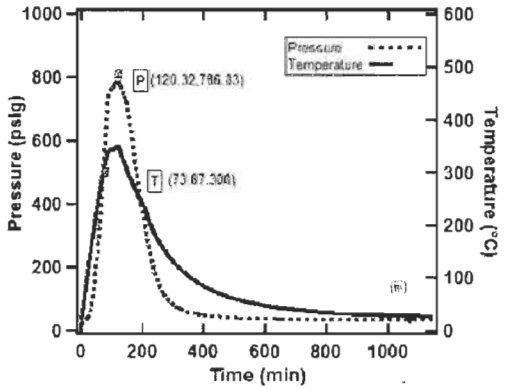
Pressure
Temperature
P (120.32,786.83)
T (73.67,300)
Pressure (psig)
Temperature (°C)
Time (min)
(iii)

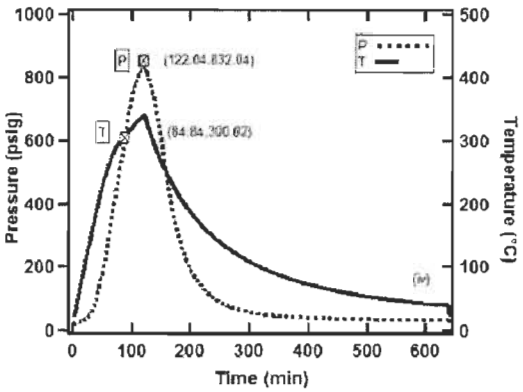
P
T
P (122.04,832.04)
T (84.84,300.62)
Pressure (psig)
Temperature (°C)
Time (min)
(iv)

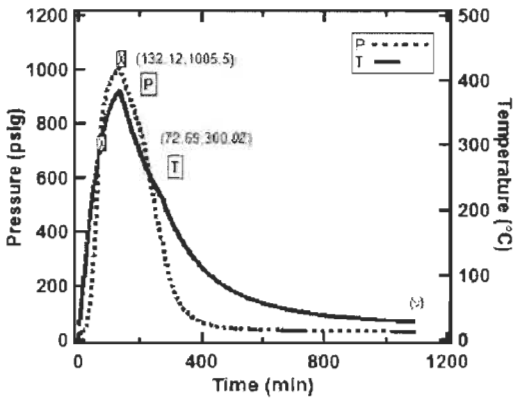
P
T
(132.12,1005.5)
P
(72.69,300.02)
T
Pressure (psig)
Temperature (°C)
Time (min)
(v)

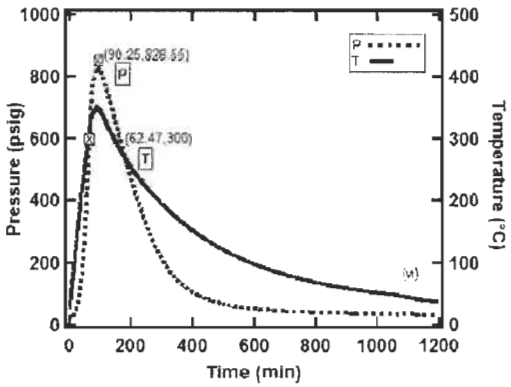
P
T
(90.25,826.55)
P
(62.47,300)
T
Pressure (psig)
Temperature (°C)
Time (min)
(vi)

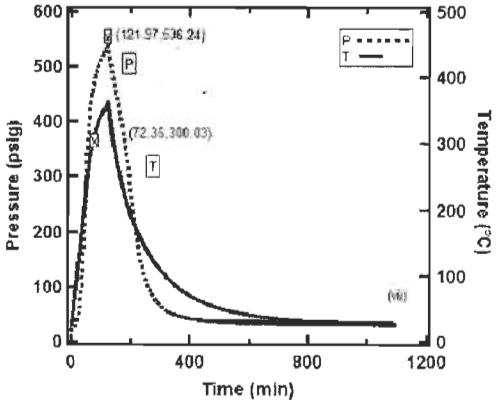

Figure 12: Pressure and temperature behaviour in run (i), run (ii), run (iii) ,run (iv), run (v) , run (vi) and run (vii).

run (i-ii) - pure Ni, run
(iii-vii) - supported Ni

Table 2 provides a summary of the runs performed with the cellulose feed, NaOH concentration and the type of Ni catalyst used. It also provides temperature and pressure readings before and after the gasification. The standard deviation is 1.3 for the pressures and temperatures. Initial pressure is the pressure inside the reactor before the start-up and final pressure is the maximum pressure produced by reforming and cool down pressure is the pressure after the reactor is cooled back to room temperature. The reactor was cooled down to condense the water vapor formed and hence to eliminate the pressure contributions from water vapor and nullify the pressure due to Ar expansion at high temperature. An increase in pressure from the initial pressure was noticed in sample runs conducted with catalysts [runs (i-vii)] compared to the run without catalyst. The cool down pressures vary from 26-31 psig for the sample runs; the lower pressure (26 psig) being attributed to the run using pure Ni catalyst.

Blank runs were also conducted using Cellulose and water [run (ix)] as well as with NaOH and water [run (x)].In both the cases the cool down pressures (21.78 psig, 20.57 psig) reverted to the initial pressure of the reactor which infers there was no effective gas production during the gasification. Re-run sample [run (xi)] is the gasified sample which has been further heated to 300 °C after the addition of 50% of initial NaOH mass. We found no increase in pressure for the re-run sample which shows that sample which has been reformed once cannot undergo further gasification to produce hydrogen.

A sample run [run (xii)] was even conducted under lower temperature (104° C) and it was found that no chemical reaction has occurred at this temperature and the sample remained

intact inside the reactor. The temperature 104 °C was chosen due to the elevation in boiling point of the water due to the presence of dissolved sodium hydroxide.

Table 2 – Summary of the experimental runs in Alloy – 600 batch reactors.

Sample Runs	Cellulose	Catalyst	NaOH		Pressure (psig)			Temperature(°C)		
	Mass (g)	Mass (g)	Molarity (M)	H_2O (mL)	Initial (Ar)	Final	Cool down	Initial	Final	Cool down
Sample Run (i)	1	Ni pure : 0.26	2	37	20.55	862.05	26.59	25.79	382.91	27
Sample Run (ii)	1	Ni pure : 0.26	4	18.5	20.47	524.36	29.26	23.16	370.99	25.50
Sample Run (iii)	1	Ni sup: 0.4	2	37	21.01	786.04	31.35	22.16	349.83	26.12
Sample Run (iv)	1	Ni sup: 0.4	2	37	20.22	832.96	28.94	23.35	339.61	24.82
Sample Run (v)	1	Ni sup: 0.4	2	37	20.45	1005.50	30.81	22.89	383.41	27.48
Sample Run (vi)	1	Ni sup: 0.4	4	37	20.81	828.55	28.51	23.58	350.51	28.62
Sample Run (vii)	1	Ni sup: 0.4	4	18.5	20.03	536.35	29.84	23.85	361.62	25.51
No catalyst run (viii)	1	-	2	37	20.43	816.04	22.82	23.69	326.97	25.10
Blank Run (ix) Cellulose+H_2O	1	-	-	37	20.68	869.42	21.78	23.07	311.13	24.44
Blank Run (x) NaOH+H_2O	-	-	2	37	20.55	832.19	20.57	23.40	23.8	24.8
Re-run Sample (xi)	1	Ni pure : 0.26	4	18.5	20.21	350.69	20.76	24.42	339.13	23.61
Low temp Sample run (xii)	1	Ni sup: 0.4	2	37	20.63	41.39	21.59	27.77	104.8	37.13

The gas produced in sample runs conducted in presence of catalyst was analyzed using MicroGC 3000 and Table 3 provides the gas composition data. It was found that hydrogen constitutes about 95% of the gas produced in runs performed with supported Ni catalyst and 79% in sample run with pure Ni catalyst and 2 M NaOH and 95% with pure Ni and 4 M NaOH. The presence of O_2 and N_2 in the gas analysis was due to an air leak detected in MicroGC and a small quantity of methane (CH_4) was also formed during the gasification. Figure 13 shows the chromatogram of the gas analysis of a typical run and the peaks have been labeled.

Table 3- Gas Chromatography analysis data

Sample Runs	**GC analysis (Area %)**			
	H_2	**O_2**	**N_2**	**CH_4**
Sample Run (i)	79.55	5.05	15.29	0.11
Sample Run (ii)	95.69	1.64	2.65	0.02
Sample Run (iii)	95.2	1.50	3.10	0.67
Sample Run (iv)	90.63	2.26	6.79	0.33
Sample Run (v)	96.37	1.05	1.99	0.58
Sample Run (vi)	94.36	1.57	3.51	0.56
Sample Run (vii)	94.42	1.39	2.13	1.95

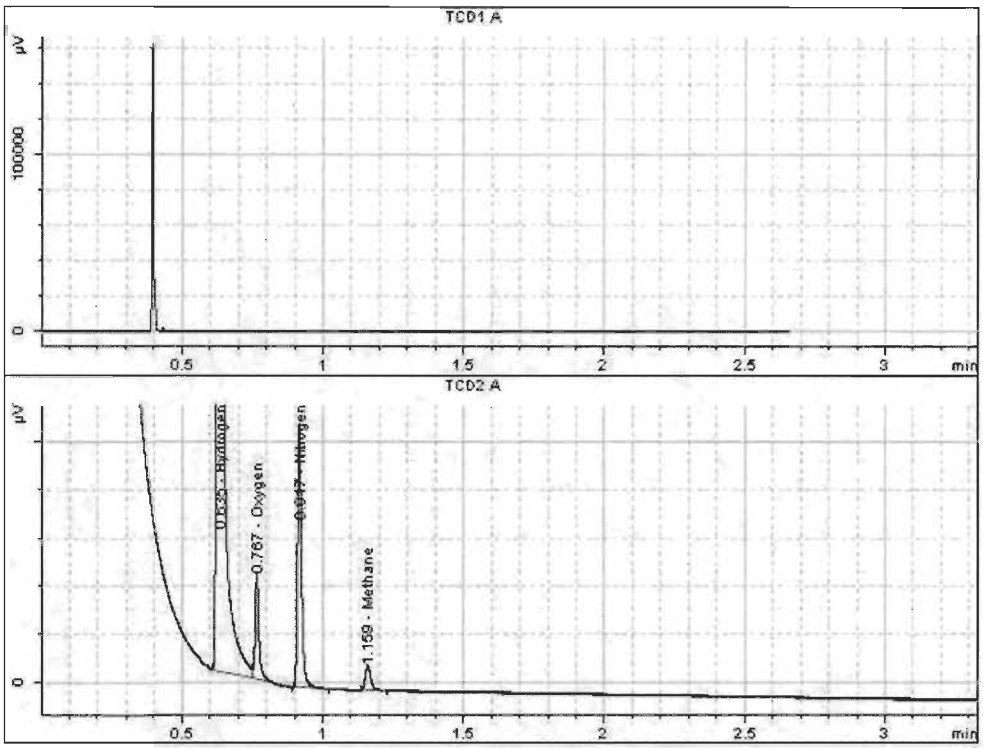

Figure 13: Gas Chromatogram of a typical run

Hydrogen mass & Efficiency calculation

The pressure rise was observed for sample runs in presence of catalysts and the GC analysis showed that H_2 constitutes $\geq$ 95% of the gas produced by aqueous alkaline reforming. The reactor was cooled down to room temperature to eliminate the pressure contribution from water vapor and Argon expansion and the mass of hydrogen formed was calculated based on the cool down pressures. The cool down pressures of the experimental runs varied from 26 psig to 31 psig for different runs.

Run (v) is taken as the sample of study and the GC analysis of run (v) shows that hydrogen constitutes 96.37 % of the total gas produced and the cool down pressure is 30.81 psig. The mass of hydrogen produced is calculated using the real gas equation,

$$PV = ZnRT, \quad (3)$$

where P is the final cool down pressure of the reactor, V is the volume of the reactor, Z is the compressibility factor, n is the number of moles of gas, R is the universal gas constant (8.314 J mol^{-1} K^{-1}), and T is the final cool down temperature. The calculation is based on the number of moles of gas present before and after the gasification run.

The number of moles of argon, n_1 were calculated based on the initial pressure (20.45 psig), reactor volume (1440×10^{-6} m^3) and initial temperature (22.89 °C) using the real gas equation. The value of the compressibility factor (Z) was obtained from the NIST table at a temperature of 22.89 °C (296.04 K) and a pressure of 20.45 psig (1 40997 Pa).The total number of moles (n_1+n_2) after cooling were calculated based on the final cool down pressure (30.81 psig), where n_2 denotes the number of moles of H_2. The value of the compressibility factor (Z) is obtained from NIST table based on the mole fractions of H_2 and Ar calculated from the partial pressures. Based on the final cool down pressure, reactor volume and cool down temperature, the number of moles of hydrogen produced were found to be 0.039 mole, which constitutes 0.08 g. The mass of H_2 supposed to be obtained from 1 g of cellulose with 100% conversion is 0.1493 g. Hence the efficiency of the process is given as

$$\eta = \frac{\text{Mass of } H_2 \text{ produced by 1 g of cellulose}}{\text{Mass of } H_2 \text{ present in 1g of cellulose}} \qquad (4)$$

The efficiency of the process is found to be 53.80 % from the production of 0.08 g of H_2 from 1 g of cellulose. The drop in efficiency is due to the less efficient heating which reduces the gasification rate which in turn affects the hydrogen production rate.

Qualitative and Quantitative analysis of the by-product

The by-product solution was analyzed qualitatively using XRD and Raman spectroscopy techniques. Qualitative analysis is detailed in the paper; XRD pattern and Raman spectra of the sample solution are given in Figures 5 and 6 respectively (from the submitted paper).

The by-product solution was analyzed quantitatively using double indicator salt titration; salt solution was titrated against 0.01 M hydrochloric acid with Phenolpthalein and Methyl Orange as the two indicators. The theory of double salt indicator titration is such that it

comprises two end points; first one denotes the complete neutralization of NaOH and conversion of sodium carbonates to bicarbonates given by Phenolpthalein and the second one, which denotes the complete neutralization of sodium bicarbonates, is given by methyl orange. The concentration of NaOH was calculated from the volume of HCl obtained after the deduction of second end point volume from the first end point volume and Na_2CO_3 concentration from the volume of HCl used to obtain the second end point. The water added before the sample run was 37 mL for 1 g of cellulose and the water remained after the run was found to be nearly 30 mL. The equation:

$$C1V1=C2V2 \qquad (5)$$

was employed for the calculation and the concentration of sodium carbonate and sodium hydroxide in the by-product sample was found to be 2.67 g and 0.62 g, respectively, in 30 mL of the solution.

The Ni catalyst used in the gasification experiment was reusable and hence could be recuperated from the solution. The Ni catalysts was separated from the by-product solution using different methods such as filtration, sedimentation, centrifugation and magnetic separation. Three methods such as sedimentation, centrifugation and magnetic separation were used for the separation process of both supported Ni and pure Ni and the results are given in Table 4.

Table 4: Yield of Nickel separation process.

	Yield (%)	Time (hours)
Supported Ni (65 wt. %)		
Sedimentation	97	3.0
Centrifugation	60	1.0
Magnetic Separation	42	0.5
Ni (99.7%)		
Sedimentation	90	3.0
Centrifugation	86	1.0
Magnetic Separation	95	0.5

A high yield of separation (97%) was obtained using sedimentation method for supported Ni (65 wt.%) and using magnetic separation for pure Ni (99.7%). Sedimentation is a time consuming process (3 hours) and whereas magnetic separation is a quick process (0.5 hour). Centrifugation is the second effective choice of separation for supported Ni which has a yield of 60%, while sedimentation holds the second choice of separation for pure Ni with a yield of 90%. Centrifugation requires time duration of 1 h to obtain a good deposition. Sedimentation method being more efficient and less energy expensive could be used as a method of choice for the separation process for supported Ni and magnetic separation for pure Ni.

The by-product samples are shown in Figure 14 (Fig. 7 from the submitted paper) and it is evident that the by-product solution was more clear in the experimental runs which used supported Ni catalyst (65 wt.% Ni/Al-Si) compared to the runs which used pure Ni (99.7%) catalyst. The first sample is the run in which pure Ni was used and second and third are the samples which used the supported Ni catalyst. It could be observed the charring tendency was found to be high in the first sample which used pure Ni catalyst compared to the other two samples which used supported catalysts.

6. Conclusion

The experimental runs conducted in different reactors proved that stainless steel is not a good material of choice for hydrogen and caustic related processes. It can be highly prone to caustic and hydrogen embrittlement and stress-corrosion cracking (SCC). An alloy which has high Nickel content is a suitable material to resist the embrittlement and SCC due to the ability of Ni to form protective stable oxides and hydroxides in high pH environments which acts as a protective passive film. In general, resistance to general corrosion and stress corrosion cracking increases with nickel content. As the alloys which have high Ni content are much more expensive, a coating of Ni or Alloy-600 (Inconel) on stainless steel reactor is a suggestion to reduce the expense towards the material cost, but further experiments are required to understand the suitability.

The cartridge heaters were found to be twice as efficient as band heaters as it took only 30 min for the system to reach 300 °C, whereas with band heaters it took more than 1 h. But the insertion of cartridge heaters on reactor walls by drilling a hole affects the reactor strength and durability. Hence if the reactor material could develop with inbuilt cartridge heaters it could save high energy input to heat up the reactor. In case of band heaters selection, band heater made of suitable material of better thermal conductivity, which provides maximum heat conduction to the reactor needs to be selected. Instead of using a single band heater it could be advantageous to use multiple band heaters of same capacity for rapid heating. Heat dissipation was found to be high for tape heaters compared to the band heaters. Heat dissipation can be minimized to a greater extent by using a highly efficient insulation material for the reactor. The reactor mass or the weight of the system to be heated up should be regulated by the congruent design of the system. Bore through thermocouple welding are not preferred on the curved surface for a high pressure system. It is always recommended on the flat bottom or top surface. Torispherical headed reactors are the best to withstand high pressures and the optimum height to diameter ratio depends on the application. The reactor wall thickness should be based on the tensile strength and joint efficiency factor of the material.

10 psig of gas production, which constitutes ≥ 95% of hydrogen was obtained from 1 g cellulose biomass feedstock and the efficiency of the system was found to be 53.38%. The high pressure formation in the system was due to the presence of water, which forms water vapour during the heating process. The production of hydrogen can be improved by optimizing the amount of water addition and hence the concentration of NaOH required for the reforming reaction. Quantitative analysis using double indicator titration against conc. HCl provides the presence of 2.67 g of soda ash and 0.62 g of caustic soda in the by-product salt solution, and hence the conversion efficiency of sodium hydroxide to carbonate as 68.10%.The salt solution was qualitatively analyzed using XRD and Raman spectroscopy which identified the presence of carbonates. The by-product of gasification, soda ash is widely used in glass industries, in the manufacture of chemicals such as baking soda and other sodium containing compounds, gas desulphurization and in pulping and bleaching process in paper industries. The Ni catalyst used in the gasification process can be recuperated and reused which makes the process cost-effective. Sedimentation and magnetic separation are chosen as the best methods for the recuperation of supported Ni and pure Ni respectively.

The conversion of biomass to hydrogen and soda ash is not fully complete and hence there remains unconverted sodium hydroxide. Further studies need to be performed to study the conversion process of remaining sodium hydroxide to soda ash, optimisation of catalyst support and NaOH concentration. The efficiency of the system can be improved by increasing the heating efficiency, optimizing the NaOH concentration and the amount of catalyst feed. In addition, the process can be more economical in a continuous scale of reaction for hydrogen production in comparison to a batch process.

References

[1] http://www.epa.gov/climatechange/basics/

[2] Debabrata Das, "Hydrogen production by biologic al processes: a survey of literature", *Int. J. Hydrogen Energy* **26**:13-28(2001).

[3] Timothy Lipman, "An overview of hydrogen produc tion and storage systems with renewable hydrogen case studies", Clean Energy Stat es Alliance Report, *Renewable Energy Fuel Cell Technologies Program, US DOE, May 2011.*

[4] Elif Kırtay, "Recent advances in production of hydrogen from biomass", *Energy Conversion & Management* **52**: 1778–1789(2011).

[5] Akshat Tanksale, Jorge Norberto Beltramini, GaoQing Max Lu, "A review of catalytic hydrogen production processes from biomass", *Renewable and Sustainable Energy Reviews* **14**:166–182(2010).

[6] M. Senthil Kumar, A. Ramesh, B. Nagalingam, "Us e of hydrogen to enhance the performance of a vegetable oil fuelled compression ignition engine", *Int. J. of Hydrogen Energy* **28**: 1143 – 1154(2003).

[7] http://www.eoearth.org/article/Hydrogen_production_technology.

[8] Resini C, Arrighi L, Delgado MCH, Vargas MAL, Alemany LJ, Riani P, et al., "Production of hydrogen by steam reforming of C3 or ganics over Pd–Cu/c- Al $_2O_3$ catalyst", *Int. J. of Hydrogen Energy* **31**:13–9(2006).

[9] Trygve Riis, Elisabet F. Hagen, Preben J.S. Vie, Øystein Ulleberg, "Hydrogen Production - Gaps and Priorities", Institute for En ergy Technology, PO Box 40, NO–2027 Kjeller, NORWAY.

[10] http://www.iphe.net/docs/Events/China_9-10/1-3_2010-9-21_IPHE_PDRD.pdf

[11] S. Yolcular, "Hydrogen production for energy u se in European Union countries and Turkey", *Energy Sources, Part A: Recovery, Utilization, and Environmental Effects*, 31:15, 1329-1337, DOI: 10.1080/15567030802089615

[12] A. Demirbas, "Biofuels sources, biofuel policy , biofuel economy and global biofuel projections", *Energy Conversion and Management* **49**:2106–16(2008).

[13] Mustafa Balat, Mehmet Balat, "Political, econo mic and environmental impacts of biomass-based hydrogen", *Int. J. of Hydrogen Energy* **34**:3589-3603(2009).

[14] David B. Levin, Heguang Zhu, Michel Beland, Nazim Cicek, Bruce E. Holbei, "Potential for hydrogen and methane production from biomass residues in Canada", *Bioresource Technology* **98**: 654–660(2007).

[15] Minoru Ishida, Kiyoshi Otsuka, Sakae Takenaka, Ichiro Yamanaka, " One-step production of CO- and CO_2-free hydrogen from biomass", *J Chem Technol Biotechnol* **80**: 281–284 (2005).

[16] Jude A. Onwudili, Paul T. Williams, "Role of s odium hydroxide in the production of hydrogen gas from the hydrothermal gasification of biomass", *international journal of hydrogen energy* **34:** 5645-5656 (2009).

[17] Sushant Kumar, Vadym Drozd and Surendra K. Saxena, "Catalytic Studies of Sodium Hydroxide and Carbon-monoxide Reaction", *Catalysts* **2**:532-543(2012).

[18] Rattana Muangrat, Jude A. Onwudili, Paul T. Williams, "Influence of alkali catalysts on the production of hydrogen-rich gas from the hydrothermal gasification of food processing waste", *Applied Catalysis B: Environmental* **100**: 440–449(2010).

[19] Minoru Ishida, Sakae Takenaka, Ichiro Yamanaka, Kiyoshi Otsuka, "Production of CO_x-Free Hydrogen from Biomass and NaOH Mixture: Effect of Catalysts", *Energy & Fuels* **20**: 748-753 (2006).

[20] Naoko Akiya, Phillip E. Savage, "Roles of Wate r for Chemical Reactions in High-Temperature Water", *Chem. Rev* **102**: 2725-2750 (2002).

[21] http://en.wikipedia.org/wiki/Hydrogen_embrittlement

[22] J R Crum, L E Shoemaker, "Corrosion Resistanc e of Nickel Alloys in Caustic Solutions", Special Metals Corporation.

[23] Alloy performance guide, Rolled Alloys.

[24] Special Metals, High-Performance Alloys for Resistance to Aqueous Corrosion.

[25] C. San Marchi, B.P. Somerday, "Technical Refer ence on Hydrogen Compatibility of Materials", Sandia National Laboratories, Livermore CA.

[26] Eugene F. Megyesy, Pressure Vessel Handbook, 12th Edition.

[27] Pressure Vessels Design and Practice , Somnath Chattopadhyay.

Appendix A: Submitted paper

The paper has been submitted as a full length article to *International Journal of Hydrogen Energy* on September 13, 2013. It presents the results discussed in this thesis.

ALKALINE AQUEOUS REFORMING OF CELLULOSE TO PRODUCE HIGH PURITY HYDROGEN WITHOUT CO_x

Amala Mary Jose, Sadesh Kumar Natarajan, Jean Hamelin[1]

Institut de recherche sur l'hydrogène, Université du Québec à Trois-Rivières, 3351 boul. Des Forges, C.P. 500, Trois-Rivières (QC), Canada, G9A 5H7

Abstract

Hydrogen is produced from cellulosic biomass without any CO_x emissions using a novel aqueous alkaline reforming (AAR) technology. The principal advantage of this process is that theoretically, all the carbon in the biomass is converted into sodium carbonate (Na_2CO_3), a product of commercial value. The moisture content in the biomass feedstock does not affect the process, as water is needed during the conversion process, thus avoiding the need to dry the biomass. The runs were conducted with different concentrations of sodium hydroxide and both supported (Ni/Al-Si) and pure Ni (~ 3 micron, 99.7%) catalysts to compare the H_2 production in different conditions. The gas produced is analyzed using a gas chromatography and the number of moles of hydrogen produced is calculated using the real gas equation. Our experimental results have shown that hydrogen with a purity of 95+% has been produced with no traces of either CO or CO_2 at temperatures as low as 300 - 350 °C with 2 M NaOH in presence of supported Ni catalyst. Mass balance study is conducted by qualitative and quantitative analyses of the by-products using XRD, Raman spectroscopy and double indicator titration.

Keywords: Hydrogen production, biomass, mass balance, alkaline aqueous reforming

[1] Corresponding author: jean.hamelin@uqtr.ca

1. Introduction

There is a voluminous demand for clean energy worldwide due to the high risk of global warming coupled with accelerated depletion of fossil fuel resources. Hydrogen economy is a long term solution for the upcoming energy crisis and it paves a way for a secure energy future[1]. Hydrogen economy comprises hydrogen production, storage and use in a cost-effective way.

Hydrogen production technologies can be widely classified as thermal, electrolytic and photolytic processes[2]. Thermal process comprises hydrogen production from fossil fuels and renewable energy sources while electrolytic and photolytic process comprises hydrogen production by splitting of water using electricity and light energy respectively. In the present scenario approximately 96% of the hydrogen produced is from fossil fuels and the rest 4% through electrolysis. Hydrogen production from fossil fuels and electrolysis process deals with the demerits of CO_2 emission which contributes to global warming and high production cost respectively. The other processes for hydrogen production such as photo-electrolysis and photo-biological processes are further away from commercialisation and need additional R&D[3-5].

Hydrogen production from renewable sources such as wind, biomass and solar energy is a viable technology for clean energy which ultimately reduces the emission of greenhouse gases. Among these, biomass based hydrogen production is proven to be a highly promising technology due to its spread and wide availability[6]. Hydrogen can be produced from biomass via biological and thermochemical routes. Thermochemical process includes steam reforming, pyrolysis, supercritical water extraction and aqueous alkaline reforming. While steam reforming and pyrolysis of biomass requires extremely high temperature operating conditions, supercritical water extraction of hydrogen occurs at very high pressure. The extreme operating conditions ensure these processes to be highly energy intensive[7-8]. Aqueous alkaline reforming process is a base facilitated hydrogen production from biomass at less extreme reaction conditions than conventional reforming reactions. This technology shows a unique feature of hydrogen production without the evolution of CO_2 as all the carbon in the biomass ends up in the form of carbonates or bicarbonates[9].

The addition of alkali metal hydroxides promotes biomass decomposition and enhances hydrogen gas production via water gas shift reaction by intermediate formation of formate salts[10]. The effect of alkali metal hydroxides reaction with biomass for hydrogen production follows the order $NaOH>KOH>Ca(OH)_2>K_2CO_3>Na_2CO_3>NaHCO_3$ [11]. From the catalysts study[12] it was found that addition of metal catalysts such as Rh, Ni, Ru, or Co on various supports decreased the formation of methane and increased the formation of hydrogen. Hydrogen production initiates at temperatures as low as 300 °C due to the presence of catalyst thus making the process less energy intensive. The catalysts promote hydrogen production by the cleavage of C-H bonds of cellulose derivatives and reaction intermediates. The optimum temperature range for hydrogen production from biomass in the presence of a catalyst by aqueous alkaline reforming process is 300–350 °C as methane production occurs at a temperature above 350 °C [13]. As the hydrogen produced by the reaction between biomass and alkali is clean and of high purity, a PEM fuel cell can be integrated directly with biomass gasification process for electricity generation.

The objective of the paper is the production of hydrogen without CO_2 formation from cellulose biomass by an aqueous alkaline reforming process in the presence of a catalyst that favours hydrogen production. The paper describes the reaction between cellulose and alkali in presence of a catalyst, the complete set up and the mass balance of the reforming process. The gas produced is qualitatively analysed using gas chromatography. The number of moles of hydrogen produced is calculated using real gas equation based on the final pressure. The by-product solution was qualitatively analysed by XRD, Raman spectroscopy and measured quantitatively using double indicator salt titration. The biomass used for the production of hydrogen is de-lignified cellulose as lignin comprises most of the carbonaceous content, hydrophobic in nature and it is the most slowly decomposing component making the process energy-expensive. The cost of lignin extraction can be compensated by its market value and hence the process does not affect the hydrogen production cost.

2. Experiment

Aqueous-phase reforming of cellulose using Ni supported on Alumina-Silica (Ni/Al-Si) catalyst was carried out in a batch reactor fabricated using annealed Inconel® Alloy 600. This Ni based alloy offers high resistance to caustic stress corrosion cracking and hydrogen embrittlement. The machined reactor was fully stress-relieved at 790 °C for 4h prior to assembly, and during operation, care has been taken to keep the operating stresses to a minimum.

The reactor has dimensions of 7" height, 6" outer d iameter and 4" inner diameter which constitute a volume of 1440 mL. The reactor was closed air tight using 16 bolts with a copper gasket of thickness 2.05 mm. The lid is provided with a gas inlet through which the setup is made oxygen free by Ar purging and a gas outlet through which the product gas flows to an Agilent MicroGC 3000 for gas analysis. Pictures of the reactor are shown in Fig. 1.

The feed comprises cellulose ($C_6H_{10}O_5$), sodium hydroxide (NaOH) and water (H_2O) in presence of Nickel (Ni/Al-Si) catalyst. The stoichiometric equation for the reaction is[13]

$$(C_6 H_{10} O_5)_n + 12n\ NaOH + n\ H_2 O \rightarrow 6n\ Na_2 CO_3 + 12n\ H_2 . \quad (1)$$

The mole ratio of carbon in biomass to alkali metal hydroxide is 1:2. The ratio of biomass wt. to catalyst wt. is 2.5:1. The runs are conducted with Ni/Al-Si (65 wt.%) as well as with pure Ni catalyst (~ 3 micron, 99.7%) in two different alkaline concentrations to compare the hydrogen production in both cases.

1 g of cellulose was mixed with 2.96 g of NaOH in 37 mL of water (2 M) and 0.4 g of Ni/Al-Si catalyst. The water added was above the stoichiometric ratio to promote the gasification pathway and to reduce charring[10]. Lower concentrations of alkali metal hydroxides were chosen to avoid caustic embrittlement and stress-corrosion cracking of the reactor. The reactor is made O_2-free and pumped with 20 psig of Ar before the heating begins.

The reactor is heated using a ceramic insulated band heater (Tempco, 1300 W), which is regulated by a PID controller connected to solid state relays and the power supply. Heat dissipation is minimized to a greater extent by using Aluminium foil backed ceramic

blanket as the insulation material for the reactor. The reactor is provided with K-type thermocouples and a high temperature pressure transducer, which provides analog current (4 mA-20 mA) as the output for temperature and pressure readings respectively. The pressure transducer was calibrated for pressures from 0 psig (4 mA) to 1000 psig (20 mA). National Instruments NI 9211(4 channel Thermocouple) and NI 9207(16 channel analog input) serves as the input modules for the temperature and voltage-current combination respectively. 15 Vdc is provided as the excitation voltage for NI 9207.

The temperature of the reactor was monitored at the reactor wall and at the heating element. The pressure increases with the increase in temperature and the reactor is allowed to stand for a retention time of 30 min to 1 h once it attains a temperature of 300 °C. It took almost 1 h for the reactor to reach 300 °C from room temperature. The heating was cut off after the retention time and the reactor was allowed to cool down to room temperature to condense the water vapour formed and hence to eliminate the pressure contributions from the water vapour formation and Ar expansion at higher temperature. At room temperature the pressure difference is noted from the initial pressure of Ar and the gas produced is analysed using the MicroGC. The MicroGC is provided with a PlotU column which detects carbon dioxide, ethylene, ethane, acetylene and a Molsieve 5A column which detects neon, hydrogen, oxygen, nitrogen, methane and carbon monoxide. A schematic representation of the reactor setup is presented in Fig. 2.

3. Results & Discussions

The main objective of the project is to produce CO_2-free hydrogen from cellulosic biomass by an aqueous alkaline reforming process as described in Eq. (1). The carbonaceous content in the cellulose is converted to sodium carbonate, a product of commercial value. We were able to meet the objective to a greater extent even though further improvements are required to commercialize the technology. The results can be divided into four sections; the first section discusses about the temperature and pressure behaviour of the runs during the heating/cooling cycle of the reactor and the GC analysis of the gas produced. The next section details about the hydrogen mass and efficiency calculation. In the third section we see the qualitative and quantitative analysis of the by-products and the fourth section discuss on catalyst recuperation.

3.1. Temperature & Pressure profile of AAR

Fig. 3 illustrates the temperature and pressure profile of the runs during the heating/cooling cycle of the reactor, time taken by the reactor to attain 300 °C, the retention time of the reactor and the maximum pressure developed inside the reactor during the retention time. The required heating time of the reactor to attain 300 °C is approximately 70 min and it is allowed to stay for a retention time of 30 – 45 min during which the pressure reached 800 - 850 psig. The high pressure production is mainly due to the formation of water vapor during the heating process and hence the reactor is allowed to cool down to room temperature to eliminate the pressure contribution from water vapor and Ar expansion before the gas analysis.

Figs. 3(i) and 3(ii) are the run profiles of the gasification sample using pure Ni (~ 3 micron, 99.7%) and 2 M and 4 M NaOH respectively. The retention time for the reactor after it attained 300 °C is 33 min for run (i) with 862 psig and 48 min for run (ii) with 524 psig. The pressure is low for run (ii) as it was performed with 18.5 ml of water unlike the other runs that were carried out with 37 ml of water. Figs. 3(iii) and 3(iv) are the run profiles using Ni/Al-Si catalyst and 2M and 4 M NaOH respectively. The maximum pressure produced for runs (iii) and (iv) are 870 psig and 828 psig with a retention time of 46 min and 28 min, respectively.

Table 1 gives a summary of the runs performed with the cellulose amount, amount of catalyst added (pure or supported Ni), concentration of sodium hydroxide based on the volume of water, pressure developed and the temperature readings at the initial and final stages. Initial pressure is the pressure inside the reactor during the start-up of heating which is kept at 20 psig of Ar and final pressure is the maximum pressure developed inside the reactor after the retention time and cool down pressure is the pressure inside the reactor after it is cooled down to room temperature. The cool down pressure of the reactor is in the range of 26-30 psig.

In sample runs from (i) to (iv), which occurred in presence of catalysts, a pressure rise is observed after cool down of the reactor to room temperature whereas in run (v) with no catalyst pressure rise is very meager. This refers that the thermochemical gasification is much effective in runs with catalysts compared to the runs without any catalysts. In blank run (vi) which has only cellulose and water and in blank run (vii) which has only NaOH

and water there was hardly any pressure rise from the initial pressure. The low temperature sample is the run conducted at lower temperature (104 °C) and found no chemical reaction has occurred inside the reactor. The temperature 104 °C is chosen due to the elevation in boiling point of water due to the presence of dissolved sodium hydroxide.

Table 2 provides the gas composition data of the gas produced during the gasification process. The gas produced by the aqueous alkaline reforming of 1 g cellulose is analysed using MicroGC 3000 and found that H_2 constitutes 79% with pure Ni catalyst and 2 M NaOH and 95% with pure Ni catalyst and 4 M NaOH. In presence of supported Ni catalyst, H_2 constitutes 94% at 2 M and 4 M NaOH respectively. The presence of O_2 and N_2 in the gas analysis result is due to an air leak in GC. From the observed results, we noted a slight CH_4 formation during the gasification process. Fig. 4 shows the detected gases by the MicroGC for a typical run.

3.2. Hydrogen mass & System efficiency calculation

The mass of hydrogen formed is calculated based on the cool down pressures. The cool down pressures of the experimental runs vary from 26 psig to 30 psig for different runs. Sample run (iii) is selected as the sample of study as it is the average of three runs conducted using supported Ni catalyst. GC analysis of run (iii) shows that hydrogen constitutes 94.06% of the total gas produced and the cool down pressure is 30.17 psig. The mass of hydrogen produced is calculated using the real gas equation, $PV = ZnRT$ in which P is the final cool down pressure of the reactor, V is the reactor volume, Z is the compressibility factor, n is the number of moles of gas, R is the universal gas constant (8.314 J mol^{-1} K^{-1}) and T is the final cool down temperature. The calculation is based on the number of moles of gas present before and after the reforming process.

The number of moles of Ar, n_1 is calculated based on the initial pressure (20.56 psig), reactor volume (1440×10^{-6} m^3) and initial temperature (22.80℃) using the real gas equation. The value of the compressibility factor (Z) is obtained from the NIST table at temperature 22.80 ° C (295.95 K) and pressure 20.56 psig (141 756.20 Pa).The total number of moles (n_1+n_2) after cooling is calculated based on the final cool down pressure (30.50 psig), where n_2 denotes the number of moles of H_2. The value of the

compressibility factor (Z) is obtained from NIST table based on the mole fractions of H_2 and Ar calculated from the partial pressures. Based on the final cool down pressure (30.50 psig), reactor volume and cool down temperature (26.15 ° C), the number of moles of hydrogen produced is found to be 0.03873 moles, which constitutes 0.0780 g. The mass of H_2 supposed to be obtained from 1 g of cellulose with 100% conversion is 0.1493 g. Hence the efficiency of the process is given as

$$\eta = \frac{\text{Mass of } H_2 \text{ produced by 1 g of cellulose}}{\text{Mass of } H_2 \text{ present in 1g of cellulose}} \qquad (2)$$

The efficiency of the process is found to be 52.30% from the production of 0.0780 g of H_2 from 1 g of cellulose. The drop in efficiency is due to the less efficient heating which reduces the reforming rate which in turn affects the hydrogen production rate.

3.3. By-product Analysis

The by-product after the reforming process is qualitatively analysed using X-ray diffraction technique. The by-product sample was dried inside an oven at 150 C for 2 hour after catalyst recuperation. From Fig. 5, sample (iii) represents gasification runs performed similarly in three different days using same reactant composition and Ni/Al-Si. The XRD patterns shows that the nature of by-products formed in runs conducted in three different days coincides very well, which clearly depicts the chemical reaction proceeded in a specific pathway and formed identical products in all the runs. The presence of by-product Na_2CO_3 is shown by the black dots in the diagram which shows a good formation of sodium carbonate.

The formation of sodium carbonate was further confirmed by Raman spectroscopy which used an excitation wavelength of 633 nm and 5 mW laser power. Fig. 6 shows the Raman spectra of the by-product samples after the reforming process. Fig. 6.a is the spectra of deionized water that shows the –OH band from 3000 – 3600 cm^{-1} and Fig. 6.b is the spectra of prepared NaOH-Na_2CO_3 solution which can be treated as a blank. Sodium carbonate peak was identified at 1080 cm^{-1} and the peak in the range from 3000 – 3600 cm^{-1} comprises –OH from water as well as from NaOH. Fig. 6.c is the spectra of by-product sample from gasification which used pure Ni as the catalyst and the peak of sodium carbonate cannot be identified whereas in Fig. 6.d, which used supported Ni as

the catalyst, we could find a well identified peak of Na_2CO_3 at 1080 cm^{-1} similar to the prepared blank sample (Fig. 6.b).This infers that in presence of supported Ni catalyst, the conversion of NaOH to Na_2CO_3 is more efficient than with pure Ni catalyst during the aqueous alkaline reforming process.

The by-product samples are shown in Fig. 7 and it is evident that the solution is clear and transparent in the experimental runs which used 65 wt.% Ni/Al-Si compared to the runs which used pure Ni (99.7%) catalyst. The first sample in Fig. 7 is the run in which pure Ni has been used and second and third are the samples which used supported Ni catalyst. The charring tendency is found to be high in the first sample compared to the other two samples which used supported catalysts.

The by-product salt solution is quantitatively analysed by double indicator titration against conc. hydrochloric. Phenolphthalein and methyl orange serve as the indicators which denote the neutralisation of sodium hydroxide that remain unreacted and the neutralisation of sodium carbonate to bicarbonates as the first end point and a complete neutralisation of sodium bicarbonates as the second end point. The titration provides the amount of sodium carbonate and sodium hydroxide in 30 ml of by-product solution as 2.67 g and 0.62 g respectively which gives a conversion percentage of sodium hydroxide to carbonate as 68.10%.

3. 4. Catalyst Recuperation

The Ni catalyst used in the gasification experiment shall be re-used and hence could be recuperated from the solution. The Ni catalysts can be separated from the solution after gasification using different methods such as filtration, sedimentation, centrifugation or magnetic separation. Three methods such as sedimentation, centrifugation and magnetic separation have been practiced for the separation process of both supported Ni and pure Ni.

A high yield of separation (97%) has been obtained using sedimentation method for supported Ni (65 wt.%) and magnetic separation for pure Ni (99.7%). Sedimentation is a time consuming process (3 hours) and whereas magnetic separation is a quick process (0.5 hour). Centrifugation is the second effective choice of separation for supported Ni 45

which has a yield of 60%, while sedimentation holds the second choice of separation for pure Ni with a yield of 90%. Centrifugation requires time duration of 1 hour to obtain a good deposition. Sedimentation method being more efficient and less energy expensive could be used as a method of choice for the separation process for supported Ni and magnetic separation for pure Ni recuperation.

4. Conclusion

The process of hydrogen production from biomass is quite a reliable method to meet future energy demand especially within the realm of clean energy. Nickel containing alloys are recommended as a choice of material for reactor construction as it is the best material to resist stress corrosion cracking and caustic and hydrogen embrittlement at higher temperature. Ni provides protection by forming stable oxides and hydroxides in high pH environments which acts as a protective passive film. As the Ni containing alloys are expensive to an extent, the cost could be compromised by providing a layer of Ni coating on a stainless steel reactor. Torispherical headed reactors are the best to withstand high pressures and the optimum height to diameter ratio depends on the application. The reactor wall thickness should be based on the tensile strength and joint efficiency factor of the material.

10 psig of gas production, which constitutes 95% hydrogen is obtained from 1 g of cellulosic biomass and the efficiency of the system is found to be 52.30%. Quantitative analysis of using double indicator titration against conc. HCl provides the presence of 2.67 g of soda ash and 0.62 g of caustic soda in the by-product salt solution, and hence the conversion efficiency of sodium hydroxide to carbonate as 68.10%. The salt solution is qualitatively analysed using XRD and Raman spectroscopy which identified the presence of carbonates. The by-product of gasification, soda ash is widely used in glass industries, in the manufacture of chemicals such as baking soda and other sodium containing compounds, gas desulphurisation and in pulping and bleaching process in paper industries. The Ni catalyst used in the gasification process can be recuperated and reused which makes the process cost-effective. Sedimentation and magnetic separation are chosen as the best methods for the recuperation of supported Ni and pure Ni respectively.

The conversion of biomass to hydrogen and soda ash is not fully complete and hence there remains unconverted sodium hydroxide. Further studies need to be performed to study the conversion process of remaining sodium hydroxide to soda ash, optimisation of catalyst support and NaOH concentration. The efficiency of the system can be improved by increasing the heating efficiency, optimising the NaOH concentration and the amount of catalyst feed. In addition, the process can be economised in a continuous scale of reaction for hydrogen production in comparison to batch process.

ACKNOWLEDGEMENTS

We would like to thank the H2Can network from the Natural Sciences and Engineering Research Council of Canada for their financial aid.

References

1. Basic Research needs of Hydrogen economy. US DOE report. May 13-15 (2003). http://science.energy.gov/~/media/bes/pdf/reports/files/nhe_rpt.pdf
2. Hydrogen Production, Overview of technology options, http://www1.eere.energy.gov/hydrogenandfuelcells/pdfs/h2_tech_roadmap.pdf.
3. Cleveland CJ , Source: DOE, http://www.eoearth.org/article/Hydrogen_production_technology.
4. Balat M and Balat M, Political, economic and environmental impacts of biomass - based hydrogen. *Int J Hydrogen Energy* **34**:3589–3603 (2009).
5. Resinia C, Arrighi L, Concepción Herrera Delgadoe M , Angeles LarrubiaVargase M, Alemanye LJ, Paola Rianic *et al.*, Production of hydrogen by steam reforming of C3 organics over Pd–Cu/c- Al2O3 catalyst. *Int J Hydrogen Energy* **31**:13–9 (2006).
6. Kırtay E, Recent advances in production of hydrogen from biomass. *Energy Conversion and Management* **52**:1778–1789 (2011).
7. Milne TA, Elam CC, and Evans RJ, *Hydrogen from Biomass State of the Art and Research Challenges.* National Renewable Energy Laboratory, Golden, CO USA.http://ieahia.org/pdfs/hydrogen_biomass.pdf
8. Boukis N, Galla U, Diem V, Jesus PD, and Dinjus E, Hydrogen generation from wet biomass in supercritical water. 2nd world conference on Biomass for Energy, Industry and Climate Protection, Rome Italy, 10-14 May (2004).
9. Reichmann B and Mays W, Base facilitated production of hydrogen from biomass, US 2005/0163074 A1,Jul. 28 (2005).
10. Onwudili JA and Williams PT, Role of sodium hydroxide in the production of hydrogen gas from the hydrothermal gasification of biomass. *Int J Hydrogen Energy* **34**:5645–5656 (2009).
11. Muangrat R, Onwudili JA and Williams PT, Influence of alkali catalysts on the production of hydrogen-rich gas from the hydrothermal gasification of food processing waste. *Applied Catalysis B: Environmental* **100**: 440–449 (2010).
12. Ishida M, Takenaka S, Yamanaka I and Otsuka K, Production of CO*x*-Free Hydrogen from Biomass and NaOH Mixture: Effect of Catalysts. *Energy & Fuels* **20**:748-753 (2006).

13. Ishida M, Otsuka K, Takenaka S and Yamanaka I, One-step production of CO- and CO2-free hydrogen from biomass. *J Chem Technol Biotechnol* **80**: 281–284 (2005).

Table 1: Summary of the experimental runs in Alloy - 600 batch reactor.

Sample Run	Cellulose	Catalyst	NaOH		Pressure (psig)			Temperature (°C)		
	Mass (g)		Molarity (M)	H_2O (ml)	Initial (Ar)	Final	Cool down	Initial	Final	Cool down
(i)	1	Ni pure : 0.26g	2	37	20.55	862.05	26.59	25.79	382.91	27
(ii)	1	Ni pure : 0.26g	4	18.5	20.47	524.36	29.26	23.16	370.99	25.50
(iii)	1	Ni sup : 0.4 g	2	37	20.56	874.26	30 30.50	22.80	357.61	26.15
(iv)	1	Ni sup : 0.4 g	4	37	20.81	828.55	28.51	23.58	350.51	28.62
No catalyst (v)	1	-	2	37	20.43	816.04	22.82	23.69	326.97	25.10
Blank Run (vi)	1	-	-	37	20.68	869.42	21.78	23.07	311.13	24.44
Blank Run (vii)	0	-	2	37	20.55	832.19	20.57	23.40	23.8	24.8
Low temp run (viii)	1	Ni sup: 0.4g	2	37	20.63	41.39	21.59	27.77	104.8	37.13

Table 2: Gas Chromatography analysis data.

Sample Runs	GC analysis (Area %)			
	H_2	O_2	N_2	CH_4
(i)	79.55	5.05	15.29	0.11
(ii)	95.69	1.64	2.65	0.02
(iii)	94.06	1.60	3.96	0.52
(iv)	94.36	1.57	3.51	0.56

Figure captions

Fig. 1: Alloy-600 reactor after heat treatment.

Fig. 2: Schematic representation of the reactor setup.

Fig. 3: Pressure and Temperature behaviour in run 4 (i), run 4(ii), run 4 (iii) and run 4 (iv).

Fig. 4: MicroGC sample run.

Fig. 5: XRD scans of gasified sample using supported Ni catalyst (Ni/Al-Si).

Fig. 6: Raman spectra of (a) deionized water, (b) blank and by-product samples in presence of (c) pure Ni and (d) supported Ni catalysts.

Fig. 7: By-product samples after Ni separation.

Fig. 1: Figure 7 in the thesis

Fig. 2: Figure 8 in the thesis

Fig. 3: Figure 12 (i – iv) in the

thesis Fig. 4: Figure 13 in the thesis

Fig. 5:

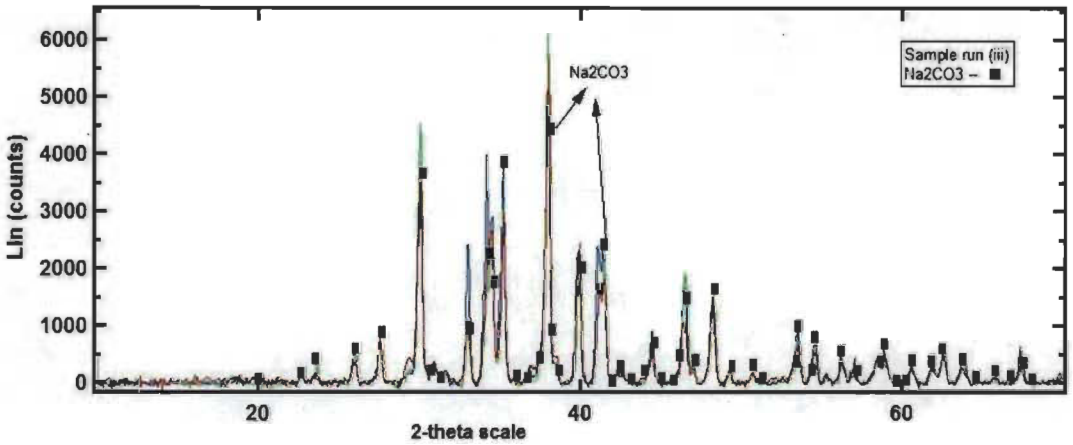

Fig. 6:

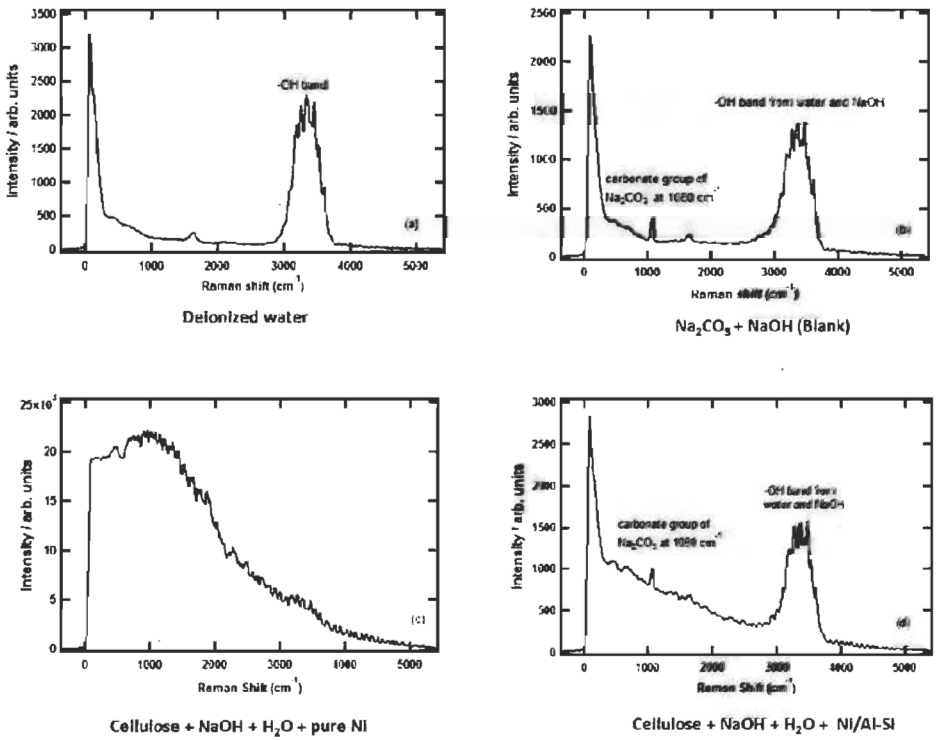

Fig. 7: